
DAP: A Dynamic Adversarial Patch for Evading Person Detectors

Amira Guesmi¹ Ruitian Ding² Muhammad Abdullah Hanif¹
Ihsen Alouani³ Muhammad Shafique¹
¹ eBrain Laboratory, NYU Abu Dhabi, UAE
² NYU Tandon School of Engineering, USA
³ CSIT, Queen’s University Belfast, UK

Abstract

Real-world physical adversarial attacks often use conspicuous and eye-catching patterns, making them easily detectable by humans. To address this, recent work has proposed using Generative Adversarial Networks (GANs) to generate naturalistic patches that may not attract human attention. However, such approaches suffer from a limited latent space making it challenging to produce a patch that is efficient, stealthy, and robust to multiple real-world transformations. In this paper, we present a novel approach for generating naturalistic adversarial patches without using GANs. Our proposed approach generates a Dynamic Adversarial Patch (DAP) that looks naturalistic while maintaining high attack efficiency and robustness in real-world scenarios. To achieve this, we redefine the optimization problem by introducing a new objective function, where a similarity metric is used to construct a similarity loss. This guides the patch to follow predefined patterns while maximizing the victim model’s loss function. Our technique is based on directly modifying the pixel values in the patch which gives higher flexibility and larger space to incorporate multiple transformations compared to the GAN-based techniques. Furthermore, most clothing-based physical attacks assume static objects and ignore the possible transformations caused by non-rigid deformation due to changes in a person’s pose. To address this limitation, we incorporate a “Creases Transformation” (CT) block, i.e., a preprocessing block following an Expectation Over Transformation (EOT) block used to generate a large variation of transformed patches incorporated in the training process to increase its robustness to different possible real-world distortions (e.g., creases in the clothing, rotation, re-scaling, random noise, brightness and contrast variations, etc.). We demonstrate that the presence of different real-world variations in clothing and object poses (i.e., above-mentioned distortions) lead to a drop in the performance of state-of-the-art attacks. For instance, these techniques can merely achieve 20% in the physical world and 30.8% in the digital world while our attack provides superior success rate of up to 65% and 84.56%, respectively when attacking the YOLOv3tiny detector deployed in smart cameras at the edge.

1 Introduction

Deep Neural Networks (DNNs) have demonstrated remarkable performance for various real-world applications and are now commonly used in safety-critical and security-sensitive domains such as video surveillance [5, 29, 23], self-driving cars [1], and health care [24]. However, studies have shown that DNNs are vulnerable to adversarial perturbations [6, 18, 25, 26]. These malicious examples can even be realized physically and deployed in the real world, posing a serious security/safety threats. There are two types of attack settings: digital attacks and physical attacks. In digital attacks [11, 6],

an attacker adds adversarial noise to the digital input image, optimized to be undetectable by human eyes while monitoring the noise budget constraint in the generation process. In contrast, in physical attacks [16, 12, 9], the attacker designs adversarial patches that are printable in the physical world and deploys them in the scene captured by the victim model. These patches are not generated under noise magnitude constraints but rather are generated under location and printability constraints, making physical patches-based attacks more practical and damaging for real-life scenarios. However, current adversarial patches are limited in the following ways:

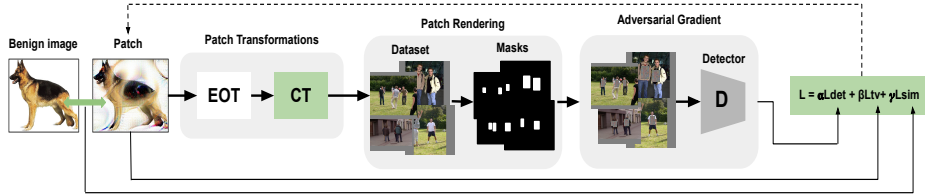


Figure 1: Overview of our dynamic adversarial patch generation framework which crafts patches that can be printed on a T-shirt and evade object detectors under different real-world conditions.

Conspicuous patterns. Previous research on adversarial patches for object/person detection [10, 31, 34] has largely focused on improving attack performance by increasing the strength of the adversarial noise. However, this approach often results in patches that are easily identifiable by human observers, limiting their effectiveness in real-world scenarios [27, 4, 13, 19]. To address this issue, some researchers have proposed using generative adversarial networks (GANs) to generate more natural-looking patches. While promising, these approaches can be inefficient (i.e., result in low attack success rate) and may not always converge to realistic/natural-looking or efficient patterns (refer to Section 3 for further details).

Assumption of static objects. Previous research assumed static objects, however, when printing an adversarial patch on a T-shirt, it is crucial to ensure that the patch is robust to additional transformations caused by changes in the fabric (e.g., deformation and orientation changes) due to a person’s movements. In particular, the constantly changing wrinkles and creases in the fabric can significantly affect the effectiveness of the attack. We demonstrate that the GAN-based techniques suffer from a limited latent vector which makes incorporating multiple transformations at once very challenging.

In this paper, we propose a novel framework (see Figure 1) to generate natural-looking adversarial patches for performing effective and robust adversarial attacks on object/person detection systems, by guiding the optimization process towards a target natural image and simultaneously maximizing the victim model’s loss. To achieve this, we propose a novel objective function that includes a similarity loss to guide the pattern of the generated noise, resulting in natural-looking patches (see Figure 4). Additionally, we incorporate a crease transformation block to model possible deformations that could occur to the adversarial patch when used to conceal dynamic objects.

Contributions – The main contributions of this paper are summarized as follows:

- We investigate the limitations of GAN-based approaches when used to generate robust naturalistic adversarial patterns, and we show that these techniques can not incorporate multiple transformations while maintaining high performance due to the limited latent space compared to the high flexibility and the larger space provided by our approach as it relies on directly manipulating the patch pixels.
- We propose a framework (See Figure 1) that generates GAN-free naturalistic patches that can resemble any predefined pattern, while maintaining high attack success rate under multiple transformations (e.g., clothing creases and wrinkles, random noise, brightness and contrast variations, re-scaling, and rotation, etc.).
- To increase robustness against non-rigid deformations experienced by a printed adversarial patch on a T-shirt and caused by pose changes of a moving person, we develop a Creases Transformation (CT) block that models these non-rigid deformations by compressing the pixels following a randomly selected direction.

- We thoroughly examine the performance/attack success rate of the proposed method in terms of mean average precision (mAP) both with and without transformations, and transferability between detectors. Our patch achieves an attack success rate of 84.56% in digital world (INRIA dataset) and 65% in the physical world when attacking the YOLOv3tiny detector for edge systems. We demonstrate the effectiveness of our patch in the digital world, when printed on a paper, and when printed on a T-shirt.

2 Related Work

Initially, physical attacks aimed at fooling person detectors were generated without considering patch stealthiness, but rather focused on performance and producing effective attacks. For example, [31] proposed printable adversarial patches attached to a cardboard, [17] proposed patches trained for random placement on the scene, and authors in [32] proposed an invisibility cloak. However, these patches had conspicuous and easily identifiable patterns. To overcome this limitation, some works proposed leveraging the learned image manifold of pre-trained GANs upon real-world images to create naturalistic patches [13, 8, 27]. Authors in [14] also proposed a universal camouflage pattern that is visually similar to natural images and for stealthiness added a L_∞ norm constraint to control the adversarial noise. These attacks were aimed to be printed on a T-shirt, but they ignored non-rigid deformations caused by a moving person. Authors in [33] attempt to model these deformations using a thin plate spline (TPS) based transformer. Nevertheless, this method ignores the stealthiness of the patch and results in conspicuous patterns. To address all these limitations and solve the trilemma of efficiency, stealthiness, and robustness, we propose an attack that generates a patch, DAP, that maintains naturalistic patterns, is robust to multiple transformations, and can be printed on a T-shirt while being stealthy. A comparison of DAP with state-of-the-art attacks is provided in Table 1.

Attack	Robustness Techniques	Stealthiness Techniques	Object	Space
Adversarial YOLO [31]	EOT, TV, NPS	-	Static	2D
Adversarial T-shirt [33]	EOT, TPS	-	Dynamic	2D
UPC[14]	EOT, TV	L_∞ norm	Static	3D
NAP [13]	TV	GAN	Static	2D
DAP (ours)	EOT, TV, CT	L_{sim}	Dynamic	2D

Table 1: DAP vs State-of-the-Art adversarial patches in terms of robustness techniques, stealthiness techniques, the targeted objects, and the Space. (EOT: Expectation Over Transformations, TV: Total Variation, NPS: Non-Printability Score, TPS: Thin Plate Spline, CT: Creases Transformation).

3 Limitations of GAN-based techniques

Authors in [13, 8, 27] proposed solving the problem of searching for naturalistic patches with adversarial effects by indirectly manipulating the latent vector z of a Generative Adversarial Network that has learnt to approach the natural patch distribution. Although GANs are known to be effective in generating images from random noise, they may suffer from multiple limitations when used to produce naturalistic patches aimed to fool object detectors that can withstand real-world distortions. In this section, we investigate those limitations.

The generator in a GAN is typically trained by sampling random vectors from a standard normal distribution, which results in a high density region centered around the origin. Thus, if the latent vector z is closer to the origin, there is a higher probability of generating realistic images, that is why a constraint τ on the norm of the latent vector z is used. In this section, we investigate the impact of incorporating multiple transformations in the naturalistic adversarial patch generation process and the impact of the norm threshold of the latent vector z on the effectiveness of GAN-based techniques for generating adversarial patches that are robust against real-world transformations. We run multiple experiments where we try to generate naturalistic patches with different combinations of transformations, i.e., without any transformations, with basic transformations (i.e. random noise, contrast and brightness variations), with basic transformations plus rotation, and when using all the transformations including the creases transformations that model wrinkles and creases in a person’s

cloth. Without loss of generality, we use the Yolov3 detector as our victim model. As illustrated in Figure 2-Left, for a norm threshold $\tau = 50$, the same value used in [13], with the increase in the number of considered transformation the effectiveness of the attack decreases. This could be explained by the fact that the latent space of the GAN is too limited to find a patch that is robust to all the basic, rigid and non-rigid transformations at once. To illustrate this, we run experiments by adjusting the norm threshold of the latent vector (i.e., $\tau = 1$ and $\tau = 100$), and report the convergence of the mean average precision (mAP) of the generated patch while training. As shown in Figure 2-Middle, corresponding to a more strict constraint, i.e., $\tau = 1$, the patch resultant patch converges to a higher mAP value leading to a lower attack success rate. We also test for $\tau = 100$, we notice that the generated patches converge to a lower mAP compared to the $\tau = 1$ case, which corresponds to a higher attack success rate. We present the final mAP for different experiments in Table 2. Figure 3 shows the generated patches for different norm thresholds, where it can be noticed that the lower the threshold the more naturalistic the generated patch looks. To conclude, the norm threshold allows a trade-off between realism and attack efficiency.

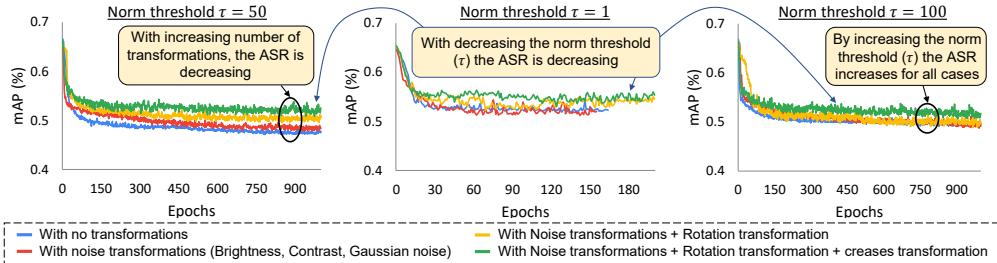


Figure 2: Mean Average Precision (mAP) convergence curves when training a GAN-based technique with and without different transformations. Illustrating the impact of adjusting the latent vector constraints on attack success rate (ASR) (Left: $\tau = 50$ (same used in [13]), Middle: $\tau = 1$, and Right: $\tau = 100$). Summary of these curves are presented in Table 2

Transformations	$\tau = 1$	$\tau = 50$	$\tau = 100$
No transformation	52.81%	47.57%	49.67%
Noise	52.55%	48.51%	49.60%
Noise + Rotation	54.05%	50.44%	49.99%
Noise + Rotation + Creases	55.16%	52.07%	51.76%



Table 2: mAP of GAN-based technique when training using different transformations.

Figure 3: Generated patches for different latent vector norm threshold.

With higher threshold, the optimization process can produce latent vectors z that are not contained within the high density region learned by the generator. Consequently, we cannot expect the generated images to look realistic. However, with lower threshold, the generated patch may look naturalistic but less effective to fool the victim detector and results in a limited latent space which decreases the tolerance to incorporating multiple transformations. Further limitations of the existing GAN-based approaches, such as failure to converge, are discussed in the supplementary material.

4 Proposed Approach

4.1 Overview

In this paper, we propose an attack that simultaneously satisfies the three key requirements needed for the adoption of adversarial attacks in the real world. These requirements include: **Effectiveness** in degrading the person detector’s performance. **Stealthiness** against human visual inspection (i.e., being unrecognizable by the observer). **Robustness** in maintaining attack ability in a dynamic environment including robustness to physical constraints. Figure 1 represents an overview of the proposed framework. We optimize the adversarial patch DAP in a way that when placed on a target object, the latter becomes undetectable by an object detector while maintaining the naturalistic pattern which will be guided by a given benign image, and being robust to real-world distortions. We achieve this by using a given benign image to guide the generation of the adversarial pattern and by

making it robust to both rigid and non-rigid transformations. To achieve this, we first apply patch transformations using the EOT and CT blocks. These blocks are used to generate a large variation of transformed patches. Then, we re-scale these patches according to the chosen scale and with respect to the sizes of people’s bounding boxes and render them on top of the input images using generated masks. The resultant adversarial images are fed into the object detector to compute different loss functions. Based on the computed gradient of the patch, we update the original patch to optimize its performance.

4.2 Attack Effectiveness

Our goal is to generate physical adversarial patches that are natural-looking while still maintaining their attack performance in real-world scenarios. We iteratively perform gradient updates on the adversarial patch (P) in the pixel space that optimizes our objective function, as defined below:

$$L_{total} = \alpha L_{det} + \beta L_{sim} + \gamma L_{tv} \tag{1}$$

L_{det} is the adversarial detection loss. L_{sim} is the similarity loss (See Section 4.3). L_{tv} is the total variation loss on the generated image to encourage smoothness (See Section 4.4). α , β , and γ are hyper-parameters used to scale the three losses. For our experiments we set $\alpha = 1$, $\beta = 4$, and $\gamma = 0.5$. We optimize the total loss using Adam [15] optimizer. We try to minimize the object function L_{total} and optimize the adversarial patch. We freeze all weights and biases in the object detector, and only update the pixel values of the adversarial patch. The patch is randomly initialized. Object detectors, such as YOLO, output an arbitrary number of boxes or detections. For each detection j , the goal is to attack two quantities: its objectness probability D_{obj}^j and its class probability D_{cls}^j . Minimizing the objectness probability D_{obj}^j causes the j -th object not to get detected. Minimizing class probability D_{cls}^j causes the j -th object to get classified into the wrong class (e.g. person gets classified as a dog.). In this paper, we focus on targeting the person class, e.g., considering the ML-based smart surveillance use cases. Thus, we minimized both the objectness D_{obj}^j and class probabilities D_{cls}^j pertaining to the person class. Our adversarial detection loss is defined by: $L_{det} = \frac{1}{n} \sum_{i=1}^n (\frac{1}{\#objects} \sum_{j=1}^{\#objects} [D_{obj}^j(I_i) D_{cls}^j(I_i)])$.

4.3 Attack Stealthiness

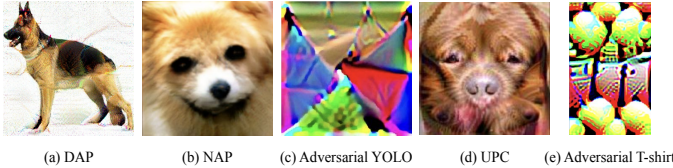


Figure 4: DAP vs State-of-the-Art patches: (a) DAP, (b) NAP (for YOLOv3tiny) [13], (c) Adversarial patch [31], (d) UPC [14], and Adversarial T-shirt [33]. Our patch is more natural looking and less conspicuous than others so it is harder to human observers to identify it

$L_{sim} = (\frac{1}{n} \sum_{i,j} (|P_{i,j} - N_{i,j}|))^2$. We square the difference between the benign image and the adversarial patch, as in quadratic functions the rate of increase (the slope or the rate of change) is slower which delays the convergence of the similarity metric with respect to the detection loss. In fact, the similarity metric is a linear function compared to the detection metric which is a nonlinear function that converges much slower. This similarity loss provides a higher flexibility compared to the GAN-based technique and the limited latent space.

4.4 Attack Robustness

Introducing the digital attack into the physical world poses an additional challenge, as the perturbation must be strong enough to withstand real-world distortions arising from variations in viewing distances

and angles, lighting conditions, camera limitations, and dynamic objects. Previous studies have revealed that adversarial examples generated via conventional techniques frequently cease to be adversarial after undergoing slight transformations [21, 20]. In order to ensure patch robustness we use two preprocessing blocks (i.e., EOT and CT blocks) to generate a large variation of transformed patches to be used in the patch training process.

4.4.1 Expectation Over Transformation (EOT)

EOT is a general framework for improving the adversarial robustness of physical attack on a given transformation distribution T [3]. Essentially, EOT is a data augmentation technique for adversarial attacks, which takes potential transformation in the real world into account during the optimization, resulting in better robustness. EOT is used to add random distortions in the optimization to make the perturbation more robust. **Spatial transformations:** The patch was randomly scaled to a size that is nearly proportional to its actual size in the scene as part of the geometric changes. Rotate the patch P at random ($\pm 20^\circ$) about the center of the bounding boxes. The aforementioned replicates printing size and location inaccuracies. **Appearance Transformations:** The pixel intensity values are altered by adding random noise (± 0.1), conducting random contrast adjustment of the value ($[0.8, 1.2]$), and doing random brightness adjustment (± 0.1) to create the color space conversions.

4.4.2 Creases Transformation (CT)

Another possible transformation when printing the generated patch on a T-shirt is constantly changing creases in the clothes resulting from a person’s movements. To overcome this challenge we perform the following transformations: A set of creases were added to the patch: Each crease was modeled by randomly selecting a point and a 2D vector (± 5) and moving all pixels in the direction of the vector, with pixels closer to the line formed by the vector extending from the chosen point moving at a greater magnitude. The movement of a point (x, y) when the chosen point is (x_0, y_0) is the vector multiplied by a multiplier, which follows the equation: $multiplier(x, y) = 1 - \frac{\sin^2 \theta [(x-x_0)^2 + (y-y_0)^2]}{width^2 + height^2}$. Where θ is the angle between the direction of the (x, y) from (x_0, y_0) and the chosen vector, and $width$ and $height$ are the dimensions of the patch.

4.4.3 Total Variation Norm (TV loss)

To increase the plausibility of physical attacks, smooth and consistent perturbations are preferred. Additionally, extreme differences between adjacent pixels in the perturbation may not be accurately captured by cameras due to sampling noise. This means that non-smooth perturbations may not be physically realizable [30]. To address these issues, the total variation (TV) [22] loss is introduced to maintain the smoothness of the perturbation. For a perturbation P , TV loss is defined as: $L_{tv} = \sum_{i,j} \sqrt{(P_{i+1,j} - P_{i,j})^2 + (P_{i,j+1} - P_{i,j})^2}$. Where the subindices i and j refer to the pixel coordinate of the patch P .

5 Experimental Setup

As victim object detectors, we used Yolov3 [28], Yolov3tiny, Yolov4 [2], and Yolov4tiny with an input image resolution of 416×416 . For the optimization, we use Adam optimizer with a learning rate of 0.001, $\beta_1 = 0.9$ and $\beta_2 = 0.999$. In our evaluations, we use the images of the INRIA [7] person dataset with pedestrians, which makes it suitable for our proposed use case setting. The dataset is popular in the Pedestrian Detection community, both for training detectors and reporting results. It consists of 614 person detections for training and 288 for testing.

6 Evaluation of attack performance

Our evaluation metric is the mean average precision (mAP), which is a commonly used performance measure in object detection tasks. To calculate mAP, we adopt the approach used in prior work [31, 13]: we take the detection boxes generated by each detector on the clean dataset as the ground truth boxes (assuming no adversarial patch is present), and then report the mAP when the same detectors are used to detect objects with the added adversarial patches. Table 5 presents the evaluation results on the INRIA dataset, where we trained our adversarial patches using four different detectors.

The victim detectors used during testing are shown in the horizontal rows, while the detectors used during training are shown in the vertical columns. As shown in the table, our approach achieves lower mAP scores across various detector combinations, demonstrating its effectiveness and transferability.

Detector	Yolov3	Yolov3tiny	Yolov4	Yolov4tiny
Yolov3	32.63%	37.13%	44.31%	38.08%
Yolov3tiny	35.93%	6.54%	43.96%	35.21%
Yolov4	50.21%	51.33%	24.65%	48.8%
Yolov4tiny	41.36%	26.47%	45.18%	16.98%

Figure 5: Attack performance in terms of mAP of DAP on INRIA dataset using different detectors.

victim detectors (64.07% attack success rate when attacking Yolov3 using a patch trained using Yolov3tiny), as evidenced by its success against models that were not used during training. This finding highlights the transferability of our approach.

6.1 DAP vs State-of-the-Art Techniques

To assess the performance of our proposed adversarial patch, we compare it against four state-of-the-art techniques: Naturalistic Patches [13], Adversarial T-shirt [33], Adversarial YOLO [31], and Universal Physical Camouflage (UPC) [14]. Table 3 summarizes the mean average precision results of these methods on the INRIA dataset. Our proposed approach achieves competitive attack performance compared to the state-of-the-art techniques. Notably, Adversarial YOLO [31] delivers the highest attack performance for most of the detectors, but the generated patches lack realism and can be easily detected due to their noticeable appearance. In contrast, our approach generates adversarial patches that blend more naturally into the surrounding while maintaining high attack performance. Overall, our approach delivers comparable performance to that of state-of-the-art techniques, while offering a more natural and subtle visual appearance.

Detector	DAP	NAP	Adversarial T-shirt	Adversarial YOLO	UPC
Yolov2	19.51%	12.06%	26%	2.13%	48.62%
Yolov3	32.63%	34.93%	-	22.51%	54.40%
Yolov3tiny	6.54%	10.02%	-	8.74%	63.82%
Yolov4	24.65%	22.63%	-	12.89%	64.21%
Yolov4tiny	16.98%	8.67%	-	3.25%	57.93%

Table 3: DAP vs State-of-the-Art adversarial patches.

6.2 Impact of adding creases on patch performance

Detector	NAP		DAP	
	w/o	w	w/o	w
Yolov3	34.93%	77.37%	32.63%	37.70%
Yolov3tiny	10.02%	69.20%	6.54%	15.44%

Table 4: Attack performance (mAP) of different Patches with and without non-rigid transformations (wrinkles).

We found that the effectiveness of the NAP was drastically degraded after applying the clothes deformation transformations. For example, the success rate of the Yolov3tiny-based NAP dropped from 89.98% to 30.8%. In contrast, our DAP patch maintained its effectiveness against the deformed clothing, with only a minor drop of 8.9% in the success rate. These results suggest that our proposed

Our experimental results, presented in Table 5, demonstrate that when using the same victim detector for training and testing, our attack achieves high performance (93.46% attack success rate when attacking Yolov3tiny). Furthermore, our technique exhibits strong transferability across different

To evaluate the robustness of different adversarial patch techniques to variations in clothing appearance, we applied random clothes deformation transformations to the INRIA dataset and measured the attack success rates. We compared the performance of our proposed DAP patch against that of the state-of-the-art Naturalistic Patches [13]. Table 4 summarizes the results.

DAP patch is more robust and less affected by variations in clothing appearance modeled by the creases in the patch compared to the state-of-the-art Naturalistic Patches.

7 Physical Attack Evaluations

7.1 Patch Performance Without Creases

To evaluate the real-world effectiveness of our proposed adversarial patch, we conducted a physical attack experiment where we printed the patch and tested its performance in a real-world setting. Specifically, we used the YOLOv3tiny-based adversarial patch shown in Figure 6. In the experiment, we took pictures of one person holding the printed patch and tested whether it could successfully evade detection by an object detector. The results of this experiment are illustrated in Figure 6, additional real-world evaluation results are provided in the supplementary materials. Our proposed patch was still effective for different distances from the camera, different angles, different scales and for different lighting conditions. Table 5 reports the detection recall in the physical world and when using our DAP, only 35% of the time a person is detected.

	Benign	NAP	DAP
Without creases	100%	30%	75%
With creases	100%	20%	65%

Table 5: Attack Success Rate (ASR) in Benign scenarios and when using DAP and NAP [13] when attacking Yolov3tiny with and without creases.



Figure 6: Detection results for different detectors, view angles, distances from the camera, patch scales, lighting conditions. Note: We had to blur the subject’s face for the blind review¹, but want to emphasize that the subject’s face in the images passed to the detector was not blurred.

7.2 Patch Performance With Creases



Figure 7: Detection results when applying random creases and rotations to the DAP patches (*left*) for Yolov3tiny and NAP patches (*right*) for Yolov3 and Yolov3tiny.

To further evaluate the robustness of our proposed adversarial patch to physical deformations, we printed the generated patch on paper and added random creases to it by crumpling this latter. As shown in Figure 7, even after being rotated, our patch was still effective in hiding the person from detection. In contrast, when we applied the same deformations to the naturalistic patches from [13] (NAP), we found that the patch was no longer effective in evading detection. This highlights the

¹The original images will be used in the final version if the paper is accepted.

strength of our proposed patch, which is more robust to physical deformations and can maintain its effectiveness even when the patch is crumpled and rotated. As shown in Table 5, the detection recall dropped to 45% even with the presence of multiple creases in the patch in addition to applying rotations.

7.3 DAP-based T-shirt

For physical attack evaluation, we also print the generated patches in 20.5cm x 21.5cm format on a T-shirt. We use Yolov3tiny to generate adversarial patches for experiments. Figure 8 illustrates the impact of our adversarial T-shirts on detection recall compared to benign ones. Our two patches succeeded in hiding the person in spite of the creases on the T-shirts.

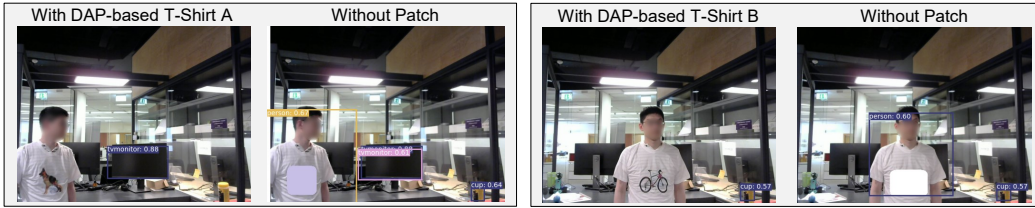


Figure 8: Detection results of with and without our DAP-based T-shirt.

8 Discussions

8.1 Impact of Patch Size

We also evaluated the patch performance with respect to the size of the target object (person). We use scales of 0.6, 0.5, 0.4, and 0.3 representing the size of the patch with respect to the size of the person bounding box (0.5 scale corresponds to 0.2 in [13]). Our experimental results, confirm that larger patches generally result in stronger attack performance, as expected. This is due to the fact that a larger patch covers more of the target object, making it more difficult for object detectors to identify the person. Overall, our experimental findings suggest that patch size is an important factor to consider when designing effective adversarial patches for object detection.

Scale	0.3	0.4	0.5	0.6
mAP	58.98%	37.20%	15.44%	6.54%

Figure 9: Attack performance against YOLOV3tiny with adversarial patches in different scales with respect to the target object size for the INRIA dataset.

8.2 Adversarial Patches in Different Classes

Our proposed adversarial patch is not limited to targeting only the "Dog" class. In fact, we were able to successfully generate effective patches for other object classes as well, such as the "Cat" and "Bike" classes. This demonstrates the versatility and potential of our approach, which can be applied to a wide range of target patterns of patch appearance. Figure 8 shows the detection results when printing the generated patches and the patches performance is summarized in Table 6. For instance, when using a Bike as the target pattern, and when applying creases to the generated patch we get 75.95% ASR.

Detector	Bike Class		Cat Class	
	w/o CT	w CT	w/o CT	w CT
Yolov3	45.46%	47.58%	38.87%	47.25%
Yolov3tiny	18.43%	24.05%	42.67%	50.05%

Table 6: DAP performance with and without transformations for the 'Bike' and 'Cat' classes for Yolov3 and Yolov3tiny detectors.

9 Conclusion

This paper presents a novel approach to generate naturalistic physical adversarial patches for object detectors. Our proposed framework overcomes the limitations of GAN-based approaches including the limited latent space, producing stealthy patches that achieve competitive attack performance. Furthermore, we introduce a creases transformation blocks to model non-rigid deformations aimed for dynamic objects. Our approach results in an effective, stealthy, and robust adversarial patch.

References

- [1] M. Al-Qizwini, I. Barjasteh, H. Al-Qassab, and H. Radha. Deep learning algorithm for autonomous driving using googlenet. In *2017 IEEE Intelligent Vehicles Symposium (IV)*, pages 89–96. IEEE, 2017.
- [2] Hong-Yuan Mark Liao Alexey Bochkovskiy, Chien-Yao Wang. Yolov4: Yolov4: Optimal speed and accuracy of object detection. *arXiv*, 2020.
- [3] Anish Athalye, Logan Engstrom, Andrew Ilyas, and Kevin Kwok. Synthesizing robust adversarial examples. In *International conference on machine learning*, pages 284–293. PMLR, 2018.
- [4] Tao Bai, Jinqi Luo, and Jun Zhao. Inconspicuous adversarial patches for fooling image-recognition systems on mobile devices. *IEEE Internet of Things Journal*, 9(12):9515–9524, 2022.
- [5] Kamel Boudjit and Naeem Ramzan. Human detection based on deep learning yolo-v2 for real-time uav applications. *Journal of Experimental & Theoretical Artificial Intelligence*, 34(3):527–544, 2022.
- [6] N. Carlini and D. A. Wagner. Towards evaluating the robustness of neural networks. *CoRR*, abs/1608.04644, 2016.
- [7] N. Dalal and B. Triggs. Histograms of oriented gradients for human detection. In *2005 IEEE Computer Society Conference on Computer Vision and Pattern Recognition (CVPR’05)*, volume 1, pages 886–893 vol. 1, 2005.
- [8] Bao Gia Doan, Minhui Xue, Shiqing Ma, Ehsan Abbasnejad, and Damith C Ranasinghe. Tnt attacks! universal naturalistic adversarial patches against deep neural network systems. *IEEE Transactions on Information Forensics and Security*, 17:3816–3830, 2022.
- [9] I. Evtimov, K. Eykholt, E. Fernandes, T. Kohno, B. Li, A. Prakash, A. Rahmati, and D. Song. Robust physical-world attacks on machine learning models. *CoRR*, abs/1707.08945, 2017.
- [10] Kevin Eykholt, Ivan Evtimov, Earlene Fernandes, Bo Li, Amir Rahmati, Florian Tramèr, Atul Prakash, Tadayoshi Kohno, and Dawn Song. Physical adversarial examples for object detectors. In *Proceedings of the 12th USENIX Conference on Offensive Technologies, WOOT’18*, page 1, USA, 2018. USENIX Association.
- [11] Ian J. Goodfellow, Jonathon Shlens, and Christian Szegedy. Explaining and harnessing adversarial examples, 2015.
- [12] Amira Guesmi, Muhammad Abdullah Hanif, and Muhammad Shafique. Advrain: Adversarial raindrops to attack camera-based smart vision systems. *arXiv preprint arXiv:2303.01338*, 2023.
- [13] Yu-Chih-Tuan Hu, Jun-Cheng Chen, Bo-Han Kung, Kai-Lung Hua, and Daniel Stanley Tan. Naturalistic physical adversarial patch for object detectors. In *2021 IEEE/CVF International Conference on Computer Vision (ICCV)*, pages 7828–7837, 2021.
- [14] Lifeng Huang, Chengying Gao, Yuyin Zhou, Changqing Zou, Cihang Xie, Alan L. Yuille, and Ning Liu. UPC: learning universal physical camouflage attacks on object detectors. *CoRR*, abs/1909.04326, 2019.
- [15] Diederik P. Kingma and Jimmy Ba. Adam: A method for stochastic optimization, 2014.
- [16] A. Kurakin, I. J. Goodfellow, and S. Bengio. Adversarial examples in the physical world. *CoRR*, abs/1607.02533, 2016.
- [17] Mark Lee and J. Zico Kolter. On physical adversarial patches for object detection. *CoRR*, abs/1906.11897, 2019.
- [18] B. Li and Y. Vorobeychik. Scalable optimization of randomized operational decisions in adversarial classification settings. In Guy Lebanon and S. V. N. Vishwanathan, editors, *Proceedings of the Eighteenth International Conference on Artificial Intelligence and Statistics, AISTATS 2015, San Diego, California, USA, May 9-12, 2015*, volume 38 of *JMLR Workshop and Conference Proceedings*. JMLR.org, 2015.
- [19] Jianyi Liu, Yu Tian, Ru Zhang, Youqiang Sun, and Chan Wang. A two-stage generative adversarial networks with semantic content constraints for adversarial example generation. *IEEE Access*, 8:205766–205777, 2020.
- [20] Jiajun Lu, Hussein Sibai, Evan Fabry, and David A. Forsyth. NO need to worry about adversarial examples in object detection in autonomous vehicles. *CoRR*, abs/1707.03501, 2017.

- [21] Yan Luo, Xavier Boix, Gemma Roig, Tomaso A. Poggio, and Qi Zhao. Foveation-based mechanisms alleviate adversarial examples. *ArXiv*, abs/1511.06292, 2015.
- [22] Aravindh Mahendran and Andrea Vedaldi. Understanding deep image representations by inverting them. In *Proceedings of the IEEE conference on computer vision and pattern recognition*, pages 5188–5196, 2015.
- [23] Akshay Mangawati, Mohana, Mohammed Leesani, and H. V. Ravish Aradhya. Object tracking algorithms for video surveillance applications. In *2018 International Conference on Communication and Signal Processing (ICCSP)*, pages 0667–0671, 2018.
- [24] R. Miotto, F. Wang, S. Wang, X. Jiang, and J. T. Dudley. Deep learning for healthcare: review, opportunities and challenges. *Briefings in bioinformatics*, 19(6):1236–1246, 2018.
- [25] A. M. Nguyen, J. Yosinski, and J. Clune. Deep neural networks are easily fooled: High confidence predictions for unrecognizable images. *CoRR*, abs/1412.1897, 2014.
- [26] N. Papernot, P. D. McDaniel, S. Jha, M. Fredrikson, Z. B. Celik, and A. Swami. The limitations of deep learning in adversarial settings. *CoRR*, abs/1511.07528, 2015.
- [27] Svetlana Pavlitskaya, Bianca-Marina Codău, and J. Marius Zöllner. Feasibility of inconspicuous gan-generated adversarial patches against object detection, 2022.
- [28] Joseph Redmon and Ali Farhadi. Yolov3: An incremental improvement. *ArXiv*, abs/1804.02767, 2018.
- [29] Alberto Sabater, Luis Montesano, and Ana C Murillo. Robust and efficient post-processing for video object detection. In *2020 IEEE/RSJ International Conference on Intelligent Robots and Systems (IROS)*, pages 10536–10542. IEEE, 2020.
- [30] Mahmood Sharif, Sruti Bhagavatula, Lujo Bauer, and Michael K. Reiter. Accessorize to a crime: Real and stealthy attacks on state-of-the-art face recognition. In Edgar R. Weippl, Stefan Katzenbeisser, Christopher Kruegel, Andrew C. Myers, and Shai Halevi, editors, *Proceedings of the 2016 ACM SIGSAC Conference on Computer and Communications Security, Vienna, Austria, October 24-28, 2016*, pages 1528–1540. ACM, 2016.
- [31] Simen Thys, Wiebe Van Ranst, and Toon Goedemé. Fooling automated surveillance cameras: adversarial patches to attack person detection. *CoRR*, abs/1904.08653, 2019.
- [32] Zuxuan Wu, Ser-Nam Lim, Larry S. Davis, and Tom Goldstein. Making an invisibility cloak: Real world adversarial attacks on object detectors. In *ECCV*, 2020.
- [33] Kaidi Xu, Gaoyuan Zhang, Sijia Liu, Quanfu Fan, Mengshu Sun, Hongge Chen, Pin-Yu Chen, Yanzhi Wang, and Xue Lin. Adversarial t-shirt! evading person detectors in a physical world. In *European Conference on Computer Vision*, 2019.
- [34] Yue Zhao, Hong Zhu, Ruigang Liang, Qintao Shen, Shengzhi Zhang, and Kai Chen. Seeing isn't believing: Towards more robust adversarial attack against real world object detectors. *CCS '19*, page 1989–2004, New York, NY, USA, 2019. Association for Computing Machinery.